

# Chapter 1

## Introduction

### 1.1 Gravitational Waves

Einstein's equations of general relativity (GR) admit radiative solutions, similar to Maxwell's equations of electromagnetism. These waves which propagate from the source to infinity with the speed of light are called gravitational waves (GWs). Unlike the case of electromagnetism, where the leading contribution to the radiated power is from the dipole, GWs are created by a time varying *quadrupole* moment. It should be noted that not only GR, but any relativistic theory of gravitation will lead to gravitational waves. However their nature and properties could be different from that in GR. The speed of GWs will depend on the details of the metric structure of the theory [1]. Theories like scalar-tensor gravity can have dipolar GWs. Unlike electromagnetic waves, for a long time there were conceptual issues related to the *physical* nature of the GWs. These doubts were cleared by the works of Bondi and collaborators [2]. They proved that gravitational waves do carry energy and angular momentum away from the system and as a result the mass of the gravitating system will decrease. Within GR, gravitational waves may be visualized as ripples in the space-time curvature. Since curvature in GR is related to the *geodesic deviation* equation (rather than the geodesic equation), just one test particle will not be sufficient to detect GWs. One would need at least two particles for the detection of GWs and conventionally it is visualized as the action of GWs on a ring of particles. The effect of GWs on a ring of particles will be to tidally distort the ring in a direction transverse to the direction of propagation. The distortion is proportional to the initial size of the ring. Thus due to equivalence principle, what is measurable are the relative distortions.

Within GR, gravitational waves are transverse and have only two linearly independent states of polarization, conventionally called 'plus' and 'cross' polarizations. Associated with each polarization state there is a time dependent gravitational field which propagates with the speed of light. In other theories of gravity, especially those which have other fields coupled

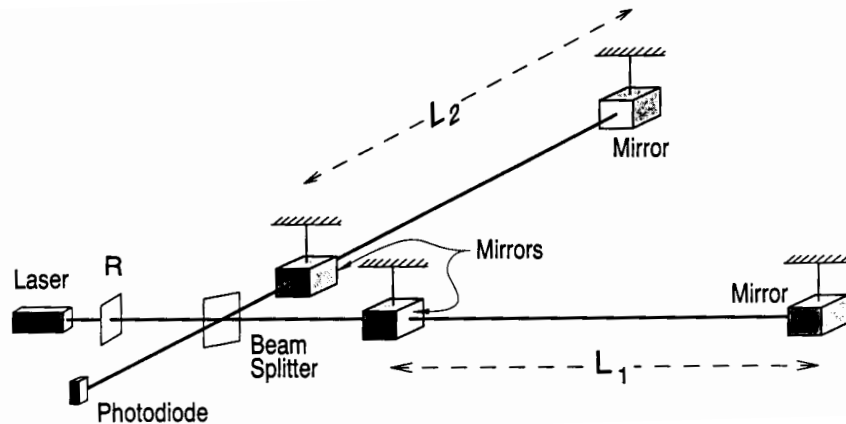


Figure 1.1: Rough schematic of a Laser interferometric GW detector. Adapted from Ref. [7].

to the metric (Brans-Dicke theory for example) GWs may not be transverse and can have up to six states of polarizations [1].

Strong experimental evidence, albeit *indirect*, exists for the existence of the GWs. This comes from the discovery observations of the binary pulsar PSR1913+16 (also known as the Hulse-Taylor pulsar) [3] (and many more binary pulsars after that) and its orbital decay. The orbital decay, due to the emission of GWs, fits very well with the predictions of GR (see [4] for an update and references therein). After the Hulse-Taylor pulsar, many pulsars have been found in binary systems and the most recent addition to the list is the double pulsar PSR J0737-3039 [5]. These open up new possibilities to explore and understand the strong field gravity regime and test GR to the highest accuracy [6] so far.

The extreme weakness of the gravitational interaction implies that a direct detection of GWs would involve the detection of very minute effects. This is a major technological challenge posed to the experimentalists. In an interferometric GW detector set up to detect GWs, one has four masses suspended from vibration-isolated supports. Two masses are near to each other on one corner of a ‘L’ shaped interferometer and one mass each at the end of the detector. Both the arm lengths are nearly equal (see Fig 1.1 for a schematic of the interferometer). When the GWs hit the interferometer, there is a change in arm-length difference which we denote to be  $\Delta L$ . This change can be monitored by the laser interferometer as function of time and one defines a quantity called strain amplitude  $h(t) = \frac{\Delta L(t)}{L}$ . Based on typical astrophysical sources, the typical strain  $h$  one has to measure in order to detect a GW is  $\sim 10^{-21} - 10^{-22}$ . In the next section we discuss the typical expected gravitational wave sources and their strain amplitudes.

## 1.2 Types of GW sources

GW sources can be very broadly classified into 4 classes: coalescence events, continuous (periodic) emitters, GW bursts and stochastic sources.

### 1.2.1 Coalescence of compact binaries

Binaries made of neutron stars (NSs) and/or black holes (BHs) are one of the most promising sources for the GW interferometers. The different phases of the coalescence of the system may be conveniently classified as *inspiral*, *merger* and *ringdown*. Using approximation schemes in GR, one can predict very accurately the waveforms associated with the inspiral and ringdown phases. Hence the most suitable data analysis strategy is to employ ‘matched filtering’ where one uses the prior information about the waveform at hand to construct templates and filters the data against a bank of templates characterized by different signal parameters. The merger phase is much more involved and a fully general relativistic treatment using numerical relativity is necessary for computing the corresponding waveforms.

The GW sources are conveniently characterized by the effective strain amplitudes they produce at the detector. Given below are the effective strain amplitudes of the inspiral sources for the ground-based and space-based detectors [8],

$$h_{\text{eff}} = 3 \times 10^{-21} \left( \frac{30 \text{ Mpc}}{r} \right) \left( \frac{\eta}{0.25} \right)^{1/2} \left( \frac{M}{2.8 M_{\odot}} \right)^{5/6} \left( \frac{1 \text{ kHz}}{f} \right)^{1/6}, \quad (1.1)$$

and for the space-based detectors

$$h_{\text{eff}} = 4 \times 10^{-17} \left( \frac{1 \text{ Gpc}}{r} \right) \left( \frac{\eta}{0.25} \right)^{1/2} \left( \frac{M}{10^6 M_{\odot}} \right)^{5/6} \left( \frac{1 \text{ mHz}}{f} \right)^{1/6}. \quad (1.2)$$

In the above expressions  $M = m_1 + m_2$  denotes the total mass and  $\eta = m_1 m_2 / (m_1 + m_2)^2$  the symmetric mass ratio.  $f$  and  $r$  refer to the frequency of the wave and distance to the source respectively.

### 1.2.2 Gravitational wave bursts

This class of events belong to the unmodelled, transient phenomena like SN explosions, Gamma Ray Bursts etc. In order to analyse the data to look for such events, one employs ‘excess power search’ methods, where one monitors power excesses in the frequency domain or looks for notable amplitude variations in time to detect a signal. Coincidence analyses involving a network of detectors will always enhance the probability of the detection. Still

one has to address the task of carefully distinguishing the spurious noise transients from an actual GW event, details of which are not relevant for the thesis and not pursued further.

The typical strain for the GW burst is [8]

$$h \sim 4 \times 10^{-21} \left( \frac{E}{10^{-7} M_{\odot}} \right)^{1/2} \left( \frac{5 \text{ ms}}{T} \right)^{1/2} \left( \frac{200 \text{ Hz}}{f} \right) \left( \frac{40 \text{ kpc}}{r} \right), \quad (1.3)$$

where  $E$  is the energy associated with the burst event,  $T$  the time of duration of the burst,  $f$  the frequency and  $r$  the distance to the source respectively.

### 1.2.3 Periodic gravitational wave sources

These sources are those which continuously emit GWs whose frequency remains constant over the duration of the observation. For the ground based detectors, spinning NSs emitting GWs by different mechanisms are examples (see Ref. [9] for a review). The two prominent mechanisms among them are

1. Normal modes as a result of residual non-axisymmetric decays
2. Accreting NS which excite non-axisymmetries (low mass x-ray binary e.g).

In the first case two important unstable modes are the  $f$ -modes and the  $r$ -modes [10, 11]. It was Wagoner [12] who pointed out that accretion could drive unstable  $f$ -modes into strong radiation. The rate of GW emission would be proportional to the accretion rate in such mechanisms.

For a non-axisymmetric NS emitting GWs at a frequency  $f$ , if  $I_{zz}$  is the moment of inertia about the spin axis of the NS, then the gravitational amplitude at a distance  $r$  is:

$$h = 3 \times 10^{-27} \left( \frac{10 \text{ kpc}}{r} \right) \left( \frac{I_{zz}}{10^{45} \text{ g cm}^2} \right) \left( \frac{f}{200 \text{ Hz}} \right)^2 \left( \frac{\epsilon}{10^{-6}} \right). \quad (1.4)$$

In the above  $\epsilon$  is the ellipticity of the NS.

The data analysis for these systems is computationally highly expensive for all-sky surveys aimed at detections of unknown pulsars [13]. More feasible are the direct searches for GW emission from known pulsars [14]. Details of these search methods are out of the scope of this thesis.

### 1.2.4 Stochastic GW background

These are ‘random’ GW signals arising from numerous uncorrelated and unresolvable sources in the sky. In particular, one is interested in the all-sky GW background similar

to the cosmic microwave background for the electromagnetic case. In the GW case, this background could arise from different physical processes in the very early universe. Observations of such a background could put severe constraints on possible ‘inflationary’ models in the very early universe.

The method by which this GW background will be looked for depends on the characteristics of the instrument. LIGO, for example, will measure the stochastic background by comparing data sets at two different sites and looking for a correlated ‘noise’ (For a review of the GWs from early universe see [15]).

## 1.3 Gravitational wave detectors

We briefly discuss the different ways to detect GWs and the frequencies at which these detectors are sensitive. GW detectors are mainly of two types: *resonant bars* and *interferometers*. Some details of these are described below. We conclude by mentioning an interesting possibility to study the GWs at very low frequencies by electromagnetic means.

### 1.3.1 Resonant bars

Historically, bar type detectors were the first to search for GWs [16]. Bars are *narrow band* instruments with a bandwidth less than 50Hz centered at around 1kHz. These are aluminium bars of length of about 3m and weighing about 1000kg. For a short burst of GW, emitted by a supernova explosion for example, the bar will have a strain sensitivity of  $\sim 10^{-21} \text{ Hz}^{-1}$ . Different bar detectors presently operational include Nautilus, Explorer and Auriga (in Italy), Allegro (in US) and NIOBE (in Australia).

We do not discuss the details of the bar detectors as this thesis deals with the other class of GW detectors, namely the laser interferometers.

### 1.3.2 Laser Interferometers

#### Ground-based detectors

These are *broad band* kilometer scale detectors sensitive to high frequency ( $\sim 10\text{-}1000\text{Hz}$ ) GWs. Different noises in different frequency ranges limit the sensitivity of these types of detectors. At low frequency ( $\sim 10\text{Hz}$ ), seismic and man-made noises limit its sensitivity, at intermediate frequencies ( $\sim 100\text{Hz}$ ) it is the thermal noise of the optical and suspended components and finally at high frequencies ( $> 300 \text{ Hz}$ ) it is the photon shot noise. Methods such as *power recycling* and *signal recycling* are employed in order to improve the detector performance.

At present there are four different interferometric detectors which are operational. In the USA, the Laser Interferometer Gravitational wave Observatory (LIGO) [17] is performing its fifth scientific run. Near Pisa, the French-Italian Virgo [18] detector is progressing fast towards its science run. The other two detectors, British-German GEO [19] and the Japanese detector TAMA [20] are also operational.

These detectors are capable of observing a wide variety of astrophysical sources (see Sec. 1.2 for details). More details of the ground based interferometers, their noise characterization which we require for our work can be found in chapter 4.

### **Space-based detectors**

These interferometers are sensitive to the low frequency ( $10^{-4} - 1$  Hz) GWs. A typical example is the proposed Laser Interferometer Space Antenna (LISA). LISA is an equilateral triangular space craft constellation, whose distance between adjacent arms is 5 million kilometers. This constellation will orbit around the sun with a  $20^\circ$  lag relative to earth. The constellation will have a tilt of  $60^\circ$  with the ecliptic plane which contains the sun and the earth.

LISA will be capable of observing the merger of binaries consisting of supermassive black holes (SMBH) and/or intermediate mass black holes (IMBH) and hence provide valuable information about BH physics and put GR to test [21, 22, 23, 24] (see Sec. 5.2.1 of chapter 5 for details of astrophysics and cosmology possible with LISA). LISA will also observe some part of the stochastic background spectrum complementing the band width over which LIGO will detect them. Unlike LIGO, LISA will probe the background GWs by combining its six data streams in an appropriate way. It can thus construct a variable that is completely *insensitive* to GWs measuring only the noise [25, 26, 27, 28]. This allows one to distinguish between noise-like stochastic background and true noise of the LISA instrument. Details of the LISA noise curve and its antenna pattern are discussed in chapter 5.

In the future, there are proposals for space-based missions entirely devoted to the stochastic background in the frequency range 0.1–10 Hz. This include Big Bang Observatory (BBO) and DECIGO [29, 30].

### **1.3.3 Electromagnetic observations of GWs**

It is interesting to note that GWs affect the electromagnetic signals and thus produce signatures measurable by observations. Prominent signals which could carry imprints of GWs are the pulsar signals and the cosmic microwave background (CMB), more specifically timing measurements of pulsars and CMB polarization measurements. We highlight them next.

#### **Pulsar Timing Arrays**

The number of millisecond pulsars detected has increased dramatically over the last few

years. A very precise timing of these pulsars could detect GW backgrounds (from SMBHs) in the nano-Hertz frequency ( $\sim 10^{-9}$  Hz) range (See Ref. [31] for a brief review). Sources in this frequency range are SMBH binaries either too massive to radiate in the LISA band or inspiralling towards the LISA band.

The effect of GWs on the pulsar timing is to create pulse period fluctuations with an amplitude proportional to the GW strain evaluated on the earth (see [32, 33] for the theoretical aspects of the problem). With the proposed Square Kilometer Array (SKA) the timing accuracy is expected to be further improved and this offers promise for GW detection. Constraints on the stochastic background in this band is likely to be better than those that can be set by any laser interferometric GW detector.

### **Cosmic microwave background polarization measurements**

The GWs produced during inflation will generate B-mode polarization in the CMB spectrum. Observing the B-mode polarization in the future CMB experiments to measure the polarization of CMB will provide useful information about the ultra-low frequency GWs in the very early universe. Ultra low frequency sources ( $10^{-18}\text{Hz} \leq f \leq 10^{-13}\text{Hz}$ ) have wavelengths of the order of Hubble length today. These waves are the result of quantum fluctuations in the early universe which are parametrically amplified during inflation to very high amplitudes. Observing the signatures of these waves could lead to better understanding of the inflationary era [34].

## **1.4 On Gravitational wave data analysis of ‘chirps’**

### **1.4.1 Matched filtering**

Matched filtering is a generalization of the pattern recognition capability of Fourier transforms (see Ref. [35] for a review). One prefers Fourier domain for performing matched filtering because of two reasons. Firstly, since the exact arrival time of the signal is not known, there will be a arbitrary time shift parameter which is naturally a shift in phase in the Fourier domain and easy to deal with. Secondly, correlation in the time domain is an optimum statistic only if the noise is *white* (independent of frequency), which is never the case. If the noise is stationary, which we assume generally for theoretical purposes, then noise at different frequencies will be uncorrelated.

The relevant details of matched filtering are discussed in chapter 4. We conclude with a few observations. Matched filter is more efficient for signals with longer duration. One has to construct very accurate templates which match with the signal over as many cycles as possible to extract out a weak short-lived signal. This is a big theoretical challenge. The computational power needed to filter such short-lived signals is also high since the number

of templates needed to effectively detect them is large. Things become even more complex if the noise is non-stationary. Details of optimal filtering are provided in chapter 4 of the thesis.

## 1.4.2 Overlaps, Effectualness and Faithfulness

A GW chirp from a nonspinning compact binary in circular orbit will be characterized by two extrinsic parameters (the arrival time and the phase of arrival) and the two intrinsic parameters (the two masses of the system). For spinning binaries spin parameters will be added to the space of intrinsic parameters. For a binary on a non-circular orbit, the eccentricity is yet another intrinsic parameter of the system.

If  $T(t; p_k)$  refers to the template and  $S(t; p_l)$  the signal, one can define the ‘overlap’ of the signal and template as [36]

$$O(T, S) = \frac{\langle T, S \rangle}{\sqrt{\langle T, T \rangle \langle S, S \rangle}}, \quad (1.5)$$

where the scalar product is defined as usual by the Wiener formula

$$\langle X, Y \rangle \equiv 2 \int_0^\infty \frac{df}{S_h(f)} [\tilde{X}(f)\tilde{Y}^*(f) + \tilde{X}^*(f)\tilde{Y}(f)]. \quad (1.6)$$

Here ‘tilde’ denotes the Fourier transform of the function; e.g.,

$$\tilde{a}(f) = \int_{-\infty}^\infty a(t) \exp(-2\pi i f t) dt. \quad (1.7)$$

In the above \* denotes complex conjugation and  $S_h(f)$  is the (one-sided) noise spectral density of the detector.

A systematic study of overlaps is possible by the introduction of a more precise characterization based on *effectualness* and *faithfulness* [36]. Faithfulness is the overlap maximised over *only* the *extrinsic parameters*. Effectualness, on the other hand, refers to the overlap which is maximised over *both* the *intrinsic* as well as *extrinsic* parameters. An effectual template is all that is required for the purpose of detection. Consequently, it is not appropriate for parameter estimation. A faithful template on the other hand implies that the biases associated with parameter estimation are also very small. Since we do not deal with detection issues or issues regarding systematic biases in parameter estimation, we will not deal with these two concepts in the rest of the thesis. The problem of parameter estimation, or the study of the statistical errors in the determination of parameters due to the noise, is what is addressed in this thesis. Relevant details of the theory of parameter estimation is provided in chapters 4 and 5.



Before proceeding to discuss other issues, it may be appropriate at this point to look into the results of the science runs of various interferometers already operational. We do this in the next section.

## 1.5 Results from the science runs of LIGO, GEO and TAMA

The results obtained from the science runs of the LIGO interferometers, GEO600 and TAMA300 are highlighted in this section.

### 1.5.1 Results from LIGO science runs

#### Search for BH inspirals in the second science run

Signatures of GW inspiral signal from binaries with total mass ranging from 3-20  $M_{\odot}$  was carried out analysing the data of the second science run of LIGO. The search was capable of detecting any BH binary up to a distance of 1Mpc with efficiency of at least 90% [37], but none were found in the 385.6 hours of data. In future this will lead to putting more interesting bounds on the event rates for the inspiral sources.

#### Search for the gravitational wave bursts

Using the data of the three LIGO interferometers during the third science run of LIGO, gravitational wave burst signals were searched in the frequency range 100 – 1100 Hz [38]. No waveform models were used and detector had an root sum square strain sensitivity of  $10^{-20} / \sqrt{\text{Hz}}$ . No gravitational waves were found in the 8 days of data that was analysed.

Another interesting burst source that was looked for was the GW signal associated with the long duration Gamma Ray Burst 030329 using LIGO detectors. Though no GW signal was detected, the root sum square gravitational wave sensitivity was better than  $6 \times 10^{-21} \text{Hz}^{-1/2}$  which is as good as the best results published in connection with the search for GWs in association with a GRB.

#### Search for stochastic gravitational wave signal

Two hundred hours of data of the 3 LIGO interferometers from the third science run were used to put limits on the GW stochastic background [39]. By searching for cross-correlations between the three LIGO detectors upper limits for energy density stored in GWs were set for three different spectral power laws. For flat spectrum the bound obtained  $\Omega_0 < 8.4 \times 10^{-4}$  in the 69-156 Hz range is  $10^5$  times better than any other earlier bounds.

#### Search for gravitational waves from known pulsars

Continuous gravitational wave signals from 28 known radio pulsars were looked for using

multi-detector analysis using the data of the second science run of LIGO [14]. Using the unprecedented sensitivity of the instrument the limits in the strain was as small as  $10^{-24}$  which translates into equatorial ellipticities of the pulsars which are smaller than  $10^{-5}$  for the four closest pulsars.

### 1.5.2 Joint searches of LIGO with other detectors

Joint LIGO-TAMA search for inspiralling NSs were carried out using a simple trigger exchange method [40]. This puts bounds on the number of coalescences with component masses between 1 and  $3 M_{\odot}$  of 49 per year per Milky Way equivalent galaxy at a 90% confidence level. Similar analysis was carried out for the burst case also [41] which looked for millisecond duration unmodelled bursts in the coincident data. The detector network was found to be sensitive to bursts with root-sum-square strain amplitude above approximately  $1 - 3 \times 10^{-19} \text{Hz}^{-1/2}$  in the frequency band 700-2000 Hz. Joint LIGO-GEO search for continuous GWs were carried out during the first and second science runs of LIGO [42]. This includes directed searches for known pulsars and blind searches for the unknown ones. Similar studies with LIGO and VIRGO are also being planned [43]

## 1.6 Different phases of binary coalescence: inspiral, merger and ringdown

Having discussed in the previous sections the different types of sources the GW interferometers will observe, we focus on the compact binary sources from now on. In the following subsections, the three phases of the binary dynamics, inspiral, merger and ringdown, are discussed and the detectability of these signals and the theoretical methods relevant for modelling them are explained.

### 1.6.1 Inspiral

This is the early stage of the dynamical evolution of the binary where it loses energy and angular momentum via gravitational radiation and spirals in. The *adiabatic* approximation, where the gravitational radiation reaction time scale is longer than the orbital time scale, is a valid approximation during this phase. This phase continues approximately all the way up to an orbital separation of  $r \simeq \frac{6GM}{c^2}$  called the last stable orbit (LSO). At the LSO, the effective potential of the system undergoes a transition from having a well-defined minimum to one without a minimum and after this point stable orbits are no longer supported. The gravitational waveform from this adiabatic inspiral is well modelled within GR using PN

approximations, where the relevant physical quantities are expressed as a perturbative series in powers of  $v/c$  (see [44] for a review).

The waveform is characterized by the two masses of the binary, the spins, some of the orbital elements of the binary and the distance to the source from the detector. The typical shape of the waveform is one which sweeps up in amplitude and frequency with time and is hence called a GW ‘chirp’. The typical frequency of the GWs during this phase is roughly given by [45]

$$f \leq 400 \left[ \frac{10M_{\odot}}{(1+z)M} \right] \text{ Hz}, \quad (1.8)$$

where  $M$  is the mass of the binary in units of solar mass  $M_{\odot}$  and  $z$  is the redshift to the source. From the above expression it is clear that typical stellar mass BH coalescences occur in the heart of the sensitivity band of the ground based detectors which have maximum sensitivity at a few hundred Hertz. On the other hand, the inspiral phase of a pair of SMBHs of  $10^6 M_{\odot}$  will emit GWs of frequency 1 mHz where the proposed space-based experiment LISA is most sensitive. Matched filtering will be employed for detection as well as parameter estimation of these binaries because one can model the waveform very accurately using approximation methods to GR.

The late inspiral, where the system moves at relativistic speeds  $\sim 0.3c$  and plunge have attracted special attention of the theorists since convergence of the PN series becomes progressively worse in this case and eventually the PN approximation breaks down. Resummation methods like Padé approximants have been suggested as a tool to improve the convergence [36, 46, 47]. The effective one body method proposed by Buonanno and Damour [48, 49] provides an analytical method to study the transition from the inspiral to plunge.

In this thesis we deal *only* with the adiabatic inspiral part, the issues related to modelling them using the PN approximation and finally studying the convergence of the PN series in the context of parameter estimation.

## 1.6.2 Merger

This is the phase beyond the adiabatic inspiral when the bodies approach and eventually cross the LSO. Modelling this phase, where the internal structure plays an important role and the approximation of point particles is no longer valid, warrants solving the full Einstein equations without any approximations. Astrophysically, if the binary is composed of two NSs, the GWs will carry information about the internal structure, equation of state and physics at very high densities which are otherwise not accessible by any other observational means.

Efforts to calculate the waveform from this phase are under way by the numerical rel-

ativists. There are two different problems numerical relativists have to tackle. The first is that of the NS-NS coalescence, which is very important not only for the GW community but also to the high energy astrophysicists because of the recent evidence that they could be the progenitors of the short duration Gamma Ray Bursts. The second is the problem of binary stellar mass BH/SMBH mergers which are of relevance to the ground-based and space-based interferometers.

In the case of binary NS simulations Ref. [50] performed a three dimensional simulation within full GR paying special attention to the resulting BH and the mass of the disk formed since it is important in the GRB context.

Recently there have been many breakthroughs in solving the binary BH problem numerically [51, 52]. Ref. [51] discussed the evolution of a binary BH based on a numerical code based on generalized harmonic coordinates. It investigated the evolution of an equal mass nonspinning binary BH through a single plunge orbit, merger and ringdown. The angular momentum parameter of the resultant BH was estimated to be  $a \approx 0.70$ . It also concluded that about 5% of the initial rest mass will be radiated during the final orbit and ringdown. Using a conformal (BSSN) formulation of Einstein's evolution equations on a cell-centered numerical grid, Ref. [52] studied the evolution in the last few orbits and merger of a binary BH system for a wide variety of initial separations. The orbits were assumed to be circular and individual masses were assumed nonspinning. The simulations resulted in the formation of a final BH with spin parameter 0.69. Plotting the frequencies as function of time, they compared the results of their simulations with that of PN theory and found excellent agreement up to 2PN.

As far as the data analysis strategies for this phase are concerned, it is instructive to employ sub-optimal methods to detect this phase and use the numerical relativity results to gain more insights into its understanding (see e.g. [53] for a discussion).

### 1.6.3 Ringdown

The last part of the compact binary evolution is when the two merged objects form a resultant BH (or a NS) and it settles to a quiescent state by radiating the deformations in the form of GWs. These gravitational waveforms can be computed using BH perturbation methods. If the newly formed compact object is a BH, then its waveform is completely determined only by its mass and the spin whereas for a NS the waveform is sensitive to the equation of state of the material. The quasi-normal-mode waveform for BHs typically has the shape of a damped sinusoid. The characteristic frequency of such sources is

$$f_{\text{QNM}} = 750 \left[ 1 - 0.63(1 - a)^{0.3} \right] (100M_{\odot}/M)\text{Hz}, \quad (1.9)$$

where  $a$  is the dimensionless spin parameter taking values in the range  $[0, 1]$ .

## 1.7 Modelling the inspiral: MPM formalism

The basic aspects the formalism we use to model the compact binary is summarized in this section. The model we follow has three parts to it. The first module is to study the motion of the compact binary and obtain equations of motion of the binary by an iteratively solving Einstein's equations in GR. The second module addresses the *generation problem*. One computes the various multipole moments associated with the compact binary by iterative solution of Einstein's equation and these moments are used to obtain the far-zone energy and angular momentum fluxes. The third part is to account for the effects of radiation reaction. One uses the expressions for the conserved energy obtained in the first module and the far-zone fluxes derived in the second and uses an energy balance argument to obtain accurate expressions for the phase  $\phi(t)$  of the binary. In the section to follow, we discuss the generation formalism in more detail.

### 1.7.1 The post-Newtonian wave generation formalism

The wave generation formalism relates the gravitational waves observed at a detector in the far-zone of the source to the stress-energy tensor of the source. Successful wave-generation formalisms mix and match approximation techniques from currently available collections. These include post-Minkowskian (PM) methods, post-Newtonian (PN) methods, multipole (M) expansions and perturbations around curved backgrounds. A recent review [44] discusses in detail the formalism we follow in the computation of the gravitational field; we summarise below the main features of this approach. This formalism has two independent aspects addressing two different problems. The first aspect, discussed in Sec. 1.7 is the general method applicable to extended or fluid sources with compact support, based on the mixed PM and multipole expansion (usually referred to as MPM expansion), and matching to some PN source. The second aspect, discussed in Sec. 1.7.3, is the application to point particle binaries modelling ICBs and issues related to regularization.

### 1.7.2 The MPM expansion and matching to a post-Newtonian source

To define the solution in the exterior of the source within the complete non-linear theory we follow Refs. [54, 55, 56, 57, 58, 59], which built on earlier seminal works of Bonnor [60] and Thorne [61], to set up the multipolar post-Minkowskian expansion. Starting from the general solution to the linearized Einstein's equations in the form of a multipolar expansion (valid in the external region), we perform a PM iteration and treat individually each multipolar piece

at any PM order. In addition to terms evaluated at one retarded time, the expression for the gravitational field also contains terms integrated over the entire past “history” of the source or *hereditary* terms. For the external field, the general method is not limited *a priori* to PN sources. However, closed form expressions for the multipole moments can presently only be obtained for PN sources, because the exterior field may be connected to the inner field only if there exists an “overlapping” region where both the MPM and PN expansions are valid and can be matched together. For PN sources, this region always exists and is the exterior ( $r > a$ ) near ( $r \ll \lambda$ ) zone. After matching, it is found that the multipole moments have a non-compact support owing to the gravitational field stress-energy distributed everywhere up to spatial infinity. To include correctly these contributions coming from infinity, the definition of the multipole moments involves a finite part operation, based on analytic continuation. This process is also equivalent to a Hadamard “partie finie” of the integrals at the bound at infinity.

The formalism, notably the asymptotic matching procedure therein, has been explored in detail and extended in a systematic way to higher PN orders [62, 63, 64, 65]. The final result of this analysis is that, the physical post-Newtonian (slowly moving) source is characterized by six symmetric and trace free (STF) time-varying moments, denoted  $\{I_L, J_L, W_L, X_L, Y_L, Z_L\}$ ,<sup>1</sup> which are specified for each source in the form of functionals of the formal PN expansion, up to any PN order, of the stress-energy pseudo-tensor  $\tau^{\mu\nu}$  of the material and gravitational fields [65]. These moments parametrize the linear approximation to the vacuum metric outside the source, which is the first approximation in the MPM algorithm. In the linearized gravity case  $\tau^{\mu\nu}$  reduces to the compact-support matter stress-energy tensor  $T^{\mu\nu}$  and the expressions match perfectly with those derived in Ref. [66].

Starting from the complete set of six STF *source moments*  $\{I_L, J_L, W_L, X_L, Y_L, Z_L\}$ , for which general expressions can be given valid to any PN order, one can define a different set of only two “*canonical*” source moments, denoted  $\{M_L, S_L\}$ , such that the two sets of moments  $\{I_L, \dots, Z_L\}$  and  $\{M_L, S_L\}$  are physically equivalent. By this we mean that they describe the same physical source, *i.e.* the two metrics, constructed respectively out of  $\{I_L, \dots, Z_L\}$  and  $\{M_L, S_L\}$ , differ by a mere coordinate transformation (are isometric). However, the six general source moments  $\{I_L, \dots, Z_L\}$  are rooted closer to the source because we know their expressions as integrals over  $\tau^{\mu\nu}$ . On the other hand, the canonical source moments  $\{M_L, S_L\}$  are also necessary because their use simplifies the calculation of the external non-linearities. In addition, their existence shows that any radiating isolated source is characterized by two and only two sets of time-varying multipole moments [61, 54].

The MPM formalism is valid all over the weak field region outside the source includ-

---

<sup>1</sup>As usual  $L = i_1 i_2 \dots i_l$  denotes a multi-index made of  $l$  spatial indices (ranging from 1 to 3). The integer  $l$  is referred to as the multipolar order.

ing the wave zone (up to future null infinity). It is defined in harmonic coordinates. The far zone expansion at Minkowskian future null infinity contains logarithms in the distance which are artefacts of the harmonic coordinates. One can define, step by step in the PM expansion, some *radiative* coordinates by a coordinate transformation so that the log-terms are eliminated [55] and one recovers the standard (Bondi-type) radiative form of the metric, from which the *radiative moments*, denoted  $\{U_L, V_L\}$ , can be extracted in the usual way [61]. The wave generation formalism resulting from the exterior MPM field and matching to the PN source is able to take into account, in principle, any PN correction in both the source and radiative multipole moments. Nonlinearities in the external field are computed by a post-Minkowskian algorithm. This allows one to obtain the radiative multipole moments  $\{U_L, V_L\}$ , as some non-linear functional of the canonical moments  $\{M_L, S_L\}$ , and then of the actual source moments  $\{I_L, \dots, Z_L\}$ . These relations between radiative and source moments include many non-linear multipole interactions as the source moments mix with each other as the waves propagate from the source to the detector. The dominant non-linear effect is due to the tails of wave, made of coupling between non-static moments and the total mass of the source, occurring at 1.5PN order ( $\sim 1/c^3$ ) relative to the leading quadrupole radiation [57]. There is a corresponding tail effect in the equations of motion of the source, occurring at 1.5PN order relative to the leading 2.5PN radiation reaction, hence at 4PN order ( $\sim 1/c^8$ ) beyond the Newtonian acceleration [56]. At higher PN orders, there are different types of non-linear multipole interactions, that are responsible for the presence of some important hereditary (*i.e.* past-history dependent) contributions to the waveform and energy flux.

A different wave-generation formalism from isolated sources, based on direct integration of retarded Einstein's equations in harmonic coordinates, is due to Will and Wiseman [67]. This provided a major improvement and elucidation of earlier investigations on the same lines [68, 61]. This formalism is based on different source multipole moments (defined by integrals extending over the near zone only), together with a different scheme for computing the non-linearities in the external field. It has currently been completed up to the 2PN order. At the most general level, *i.e.* for any PN extended source and in principle at any PN order, the Will-Wiseman formalism is completely equivalent to the present formalism based on MPM expansions with asymptotic matching (see Section 5.3 in [44] for the proof).

### **1.7.3 Applications to compact binaries: point particle binaries and regularization schemes for the self-field**

Damour [69], during his careful analysis of the Hulse-Taylor binary pulsar introduced a *matching approach* to deal with compact binaries (objects whose physical radii and gravitational radii are comparable) which consists of two parts:

1. An external perturbation scheme: an iterative weak-field (post Minkowskian) approximation scheme valid in a domain outside the world-tube of the two bodies.
2. An internal perturbation scheme: describing the small perturbations of each body by the far-field of the companion.

He showed that for compact objects the effects of internal structure of the body are *effaced* when seen in the external scheme. The effect of internal structure of the two bodies starts to appear only at 5PN order in the equation of motion. This result is the rationale for the point particle description of the compact binary.

Though treating the two compact bodies as point particles, allows a nice analytical treatment of the whole problem, it comes at the cost of handling  $\delta$ -functions in a nonlinear theory. This happens because the general formalism, described in the previous section 1.7 is set up for a smooth and continuous matter distribution and cannot be applied to point particles directly since they lead to divergent integrals at the location of the particles. Thus for using the expressions for the smooth matter distribution to the case of compact binaries we have to supplement them with a clear prescription for removing the infinite self-field of point particles.

The various regularization methods used in earlier works include Reisz regularization, Hadamard regularization, extended Hadamard regularization and more recently dimensional regularization [70, 71, 72, 73, 74, 75, 76]. At 3PN order Hadamard regularization *cannot* unambiguously regularize all the badly divergent integrals which appear and one is left with *four* ambiguity parameters. Appearance of these ambiguity parameters at a fundamental level is due to the violation of the gauge symmetry of perturbative GR in the Hadamard regularization. Recently, dimensional regularization, which respects the gauge symmetry of perturbative GR, was employed to fix these ambiguity parameters [76, 73] (see Ref. [77] for a more exhaustive reference list).

## 1.8 Inspiralling compact binaries on eccentric orbits

This section is devoted to a survey of the possible mechanisms which will produce binaries with non-negligible eccentricity and an update of the data analysis strategies in dealing with the GW signals from these sources. A detailed technical description of the theoretical inputs needed to construct the templates for eccentric binaries is in chapter 6.

### 1.8.1 Mechanisms which produce eccentric binaries

One of the most important mechanisms which could make the eccentricity of the binary non-zero, even towards late stages of their inspiral, is the Kozai mechanism [78]. Though in-



roduced in the context of asteroids in the solar systems, the mechanism involving three body interaction was found to be more general and has been studied in the context of compact binaries [79, 80, 81, 82] by Monte Carlo simulations. These works studied the dynamical evolution of a bound hierarchical triple of SMBHs in the nuclei of galaxies undergoing sequential mergers. Kozai oscillations induced on the inner binary by the outer BH can make the binary merger time substantially small. Kozai oscillations of triples in globular clusters could produce eccentric binaries in the sensitivity band of the ground based detectors whereas these oscillations in the nuclei of galaxies could produce eccentric SMBH binaries detectable by LISA.

Another scenario recently discussed is in the context of a semi-analytical treatment of the evolution of a NS-BH binary system [83]. In cases where the NS is not completely disrupted in the first phase of mass transfer, the remains of the NS could be set to move on a wider eccentric orbit. The study predicted that there could be eccentric binaries involving stellar mass NS/BH even towards late stages of inspiral. The recent SWIFT observations of GRB050911 was explained invoking the above scenario. There have been other scenarios also in the context of NS-NS and NS-BH mergers [84, 85, 86], details of which we do not discuss here. In brief, there could be a sub-class of compact binary sources, which will have non-negligible eccentricity when the GWs emitted by them enters the sensitivity band of the detectors, both ground-based and space-based.

## 1.8.2 Data analysis of GW signal from eccentric binaries

The stellar mass binaries consisting of NS and/or BH, which we discussed in the last section, are interesting sources for LISA as well and there have been studies about the necessity to model them with eccentricities. For an eccentric system, the power is spread over a large bandwidth of frequencies rather than localized at a particular dominant value of twice the orbital frequency. Consequently, the contributions from other harmonics would need to be taken into account to optimize the search templates.

Seto in Ref. [87] argued that it is possible to measure the total mass of these eccentric binaries with LISA if one includes the effect of periastron advance (which is a leading 1PN effect). Jones [88] examined the possibility of bounding the mass of graviton in massive graviton theories using eccentric binaries.

Like spin, eccentricity can also have implications for the signal-to-noise extracted by matched filtering in gravitational wave data analysis [89, 90, 91, 92, 93]. The loss of signal-to-noise ratio resulting from employing a quasi-circular orbit template to detect the signal from a binary moving in a quasi-elliptical orbit was discussed in [91]. The loss would increase with the eccentricity of the system for a fixed mass but decrease with the mass of the

system for a fixed eccentricity. Further due to the more rapid evolution of the system in the presence of eccentricity, a circular orbit template would estimate the parameters of the binary wrongly. The parameter most affected could be chirp mass which would be overestimated. This is because an increase in the chirp mass would enhance the orbital evolution mimicking the effect of orbital eccentricity [91]. Ref. [93] investigated the implications of including the harmonics of the eccentric binaries when the fundamental frequency is below the cut-off frequency from galactic confusion noise. Inclusion of the other harmonics not only improves the SNR but also gives a better estimation of the angular resolution of the binaries whose orbital periods are larger than 2,000 seconds.

A related scenario where modelling the eccentricity of the binary is important is the ‘foreground’ subtraction problem for advanced space based detectors. Recently Cutler and Harms [94] analysed the NS binary subtraction problem in the context of Big Bang Observer (BBO) estimating the effect of eccentricity. They conclude that the effects of higher harmonics should be carefully accounted to construct an efficient subtraction scheme.

In connection with the astrophysical paradigm discussed above where the assumption of vanishing eccentricity is grossly incorrect, one may need to include orbital eccentricity as an essential parameter on equal footing with the masses and spins in the data analysis. In this thesis we compute the instantaneous contribution to the 3PN angular momentum flux for eccentric binaries and apply it to discuss the evolution of orbital elements for binaries in eccentric orbits under 3PN gravitational radiation reaction in chapter 6. This would form the basis for any attempt to incorporate higher PN corrections to the data analysis problem specifically addressing the eccentric binaries.

## **1.9 Gravitational waves from compact binary inspiral: issues related to waveform modelling**

Having discussed the essential features of the three phases of compact binary evolution, we list the most important issues in modelling this system and the progress made in addressing them. This section will be used to emphasize the issues related to waveform modelling which are relevant to this thesis.

### **1.9.1 Model for the orbit of the binary: circular vs elliptic orbits**

GWs emitted by a compact binary system are detectable by ground-based and/or space-based interferometers towards the last stages of its inspiral. As shown in [95], even if the binary has eccentricity when it was formed, radiation reaction effects will circularize the orbit by the time the binary coalesces. Hence most, if not all, of the sources which will be detected

by the GW detectors will be moving in circular orbits. This realization has simplified the data analysis strategies considerably as circular orbit binaries are characterized by a smaller number of parameters as opposed to the eccentric ones.

Significant progress has been made towards the construction of templates for these binaries and waveforms have been computed, for nonspinning binaries of arbitrary mass ratio, up to 3.5PN [96, 97, 98, 99, 100] in the phase and 2.5PN in the amplitude [101, 102]. Several accuracy analyses [103, 104, 105, 36, 46, 47, 106] showed that though the 1.5PN and 2PN phasing may not be good enough for an accurate detection and parameter estimation, the 3.5PN should be reasonably accurate for the purpose.

The performance of 3.5PN templates for parameter estimation of a nonspinning binary is one of the important issues addressed in this thesis. The analytical computation of the 2.5PN accurate GW amplitude for nonspinning binaries moving in circular orbits is another important investigation of the thesis.

Though most of the binaries will be in circular orbits by the time the interferometers observe them, there could be a subclass of sources which may still have non-negligible eccentricity (see Sec 1.8 for more details). Data analysis strategies for these binaries are more involved. Equivalent to the phasing formula for the circular case, one is interested in computing how the elements of the ellipse describing the binary's orbit evolve with time. The evolution of these orbital elements can be expressed in terms of the energy and angular momentum losses of the system via GWs. The corresponding fluxes of energy and angular momentum and the corresponding orbital evolution are currently available only up to 2PN accuracy [107, 108, 109, 110, 111, 112, 113].

The instantaneous terms in the angular momentum flux at 2.5PN and 3PN orders are computed in this thesis and averaged over an orbit. This is employed to evaluate the evolution of orbital elements under gravitational radiation reaction. The energy flux up to 3PN comes from Refs [114, 115]. One has to supplement the present calculation by the evolution of the orbital elements under 'hereditary' terms at 2.5PN and 3PN in order to complete the problem up to 3PN. This complete 3PN angular momentum flux and evolution of orbital elements under GW radiation reaction will be necessary for constructing a 3PN accurate GW phasing in the future.

## **1.9.2 Assumption about the spin of the binary: spinning vs nonspinning cases**

Though one may argue that the spin effects are more important for binaries with large mass ratio, including the spin effects is an important step towards constructing more realistic and general templates. Theoretically, computation of waveforms with spin effects is more com-

plex. Till date spin effects are computed in the phase up to 2.5PN order [116, 117, 118, 119] and in the amplitude up to 2PN order [118, 120]. Ref. [116] gave a prescription to incorporate orbital precession effects and the consequent modulations in the model of the gravitational waveform.

Throughout this thesis we deal only with *nonspinning* binaries and do not address the issues related to spin at all.

### 1.9.3 Fourier domain waveform: restricted waveform vs full waveform

Further to the assumptions on a model of the orbit and the binary’s spin, analytical expressions for the Fourier domain waveform which are employed to construct templates for data analysis, use the ‘restricted waveform approximation’. The usual waveforms routinely employed in analysing the data use a very high PN accurate phasing of the binary, keeping the amplitude of the wave to be at leading Newtonian order [96]. This is justified by the argument that the matched filtering is more sensitive to the phase of the GW than its amplitude.

There have been investigations about the validity of the restricted waveform approximation in the detection as well as parameter estimation contexts [121, 122, 123, 124, 125, 126]. These analyses evaluated the differences arising by the use of the non-restricted waveform in both detection as well as parameter estimation. The overestimation in SNR by the restricted waveform templates due to the absence of higher harmonics have to be accounted for while constructing the templates for data analysis [125, 126].

As part of the thesis (chapters 2 and 3), we provide the complete 2.5PN GW polarizations for inspiralling compact binaries in circular orbits. In view of the recent developments mentioned earlier we expect our calculation to be important for the data analysis of both ground-based and space-based detectors.

### 1.9.4 Modelling the late inspiral: adiabatic vs non-adiabatic waveforms

The computation of the waveforms for the inspiralling compact binary systems are implemented using the PN approximation to general relativity. One assumes here that though the orbital frequency of the system changes with time, the change in frequency per orbital period is negligible compared to the orbital frequency itself, i.e.,  $\frac{\dot{\omega}}{\omega^2} \ll 1$ . Strictly speaking, this *adiabatic approximation* is valid only in the early part of the inspiral and not during the very late inspiral and merger phases. Hence the standard PN approximation is expected to break down towards the very late part of the inspiral.

Alternatives have to be explored to include the effects of non-adiabaticity and to model the plunge and merger phases. The effective one body (EOB) approach [48, 49, 127, 128]

first proposed by Buonanno and Damour is one of the most important among them. This method uses the Hamilton-Jacobi formalism to map the conservative dynamics of the two body problem involving two masses  $m_1$  and  $m_2$  into an *effective one body* problem of a test particle of mass  $\mu = M\eta$ , where  $M = m_1 + m_2$  and  $\eta = m_1 m_2 / M^2$ , moving in an effective background metric which is a deformed Schwarzschild metric with a deformation parameter  $\eta$ . This description of the conservative dynamics is supplemented by an additional radiation reaction force obtained from Padé resummation of the GW flux. This method, for the first time, does not assume adiabaticity anymore and provides an analytical description of the transition from plunge to merger and subsequent ‘ringing’.

Other approaches to go beyond the adiabatic approximation, have been made by Buonanno *et al* [129, 130, 131, 132] and Ajith *et. al* [133, 134]. Buonanno *et al* used a variant of the non-adiabatic model using an effective Lagrangian constructed in the PN approximation. Ajith *et al* proposed a new class of templates (*complete* non-adiabatic approximants) that reinstate the ‘missing’ conservative terms in the acceleration at 1PN and 2PN and consequently improve the standard adiabatic treatment.

With the recent progresses in numerical relativity, there is hope that one will have better waveforms for the late inspiral and merger parts of the binary evolution which can be used for constructing templates as well as to test the robustness of the analytical adiabatic and non-adiabatic models.

Throughout this thesis we work *only* within the adiabatic approximation.

### 1.9.5 Convergence of the PN series

The post-Newtonian expansion is an asymptotic expansion in the set of gauge functions  $c^{-n}(\log c)^m$ . It converges slowly and hence the rate of convergence of the PN series is a practical issue to deal with in data analysis, both for detection and parameter estimation. There have been many studies examining this aspect in the arbitrary mass ratio case and in the test mass limit. In the latter case, its even more interesting as there are exact expressions for the energy function (analytical) and flux function (numerical) which are the two crucial ingredients for constructing the phase evolution.

One method to examine the convergence of the series is to examine the total number of GW cycles each PN order contributes and investigate whether they show a convergent behaviour as we go to high PN orders [135, 105, 98, 99]. These works showed that the number of cycles arising from higher PN orders do get smaller but follow an oscillatory pattern, characteristic of the PN series. In Ref. [46], the authors introduced a more precise definition for number of cycles by weighing it by the noise PSD of the detector and termed it *number of useful cycles*. Details of this are discussed in chapter 4

Another method, more instructive from the data analysis point of view, is to calculate the ‘overlap’ between the PN template of a particular order with the exact (in the test particle case) or fiducial exact (arbitrary mass ratio case) templates which are considered to be the best representation of the actual signal. Studies in Refs [136, 36, 46, 47, 137, 133, 129, 130] also showed similar trend as for the number of cycles. More specific measures were defined specific to the problem of detection (effectualness) and parameter estimation (faithfulness) that allowed one characterize the biases in parameter estimation [36, 46, 47, 129, 130, 133].

A similar study in the parameter estimation context is lacking at present. Studies of [104, 105] compute errors associated with the estimation of the signal parameters only up to 2PN order. In this thesis, we extend this analysis including the higher order terms available at present and examine the convergence of the PN series in the parameter estimation context for the ground-based GW detectors and LISA cases. The results of this study suggest that using the 3.5PN phasing is important in both the cases to avoid systematic errors from the neglect of higher order terms.